

Supporting Information

Harnessing Nanoreactors: Gelatin Nanogels for Human Therapeutic Protein Delivery

Jeehye Kim ¹, Caroline E. Copeland ¹, and Yong-Chan Kwon ^{1,2,*}

¹ Department of Biological and Agricultural Engineering, Louisiana State University, Baton Rouge, LA 70803, USA

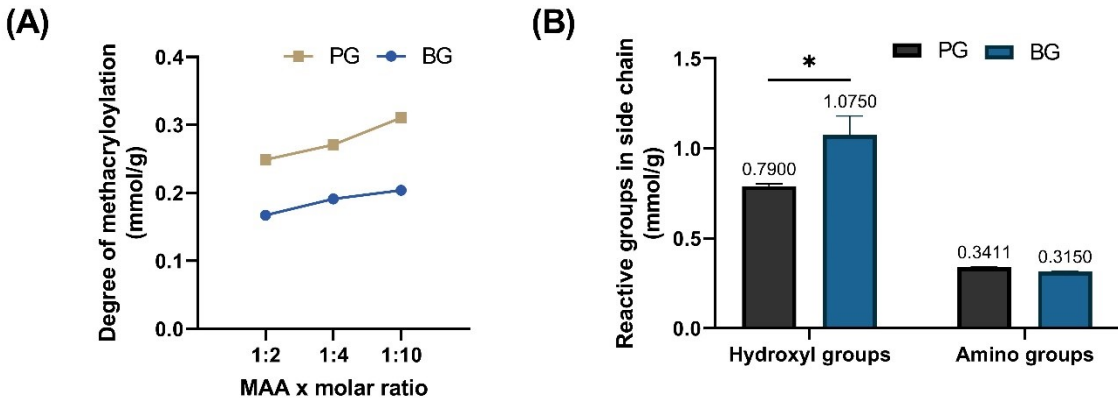
² Louisiana State University Agricultural Center, Baton Rouge, LA 70803, USA

* Corresponding author E-mail: yckwon@lsu.edu (Yong-Chan Kwon)

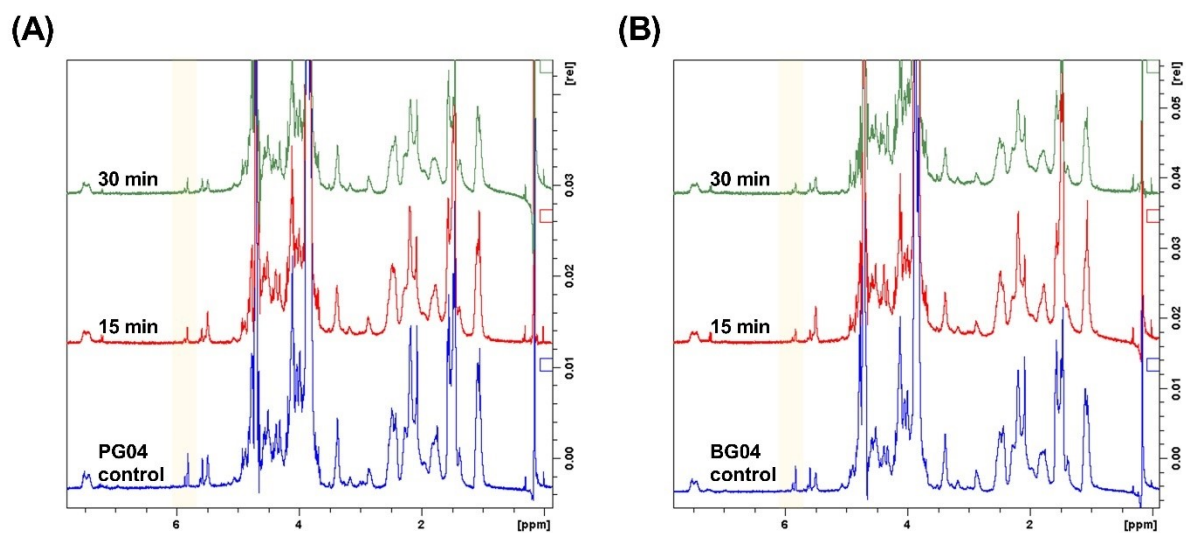
Supplementary Table S1. Reagent composition for gelatin methacryloylation reaction

Samples	ml/g gelatin	x molar ratio^a	gelatin	PBS	volume MAA
P-/BGM1	0.048	1	12.5 g	100 ml	0.6 ml
P-/BGM2	0.104	2	12.5 g	100 ml	1.3 ml
P-/BGM4	0.2	4	12.5 g	100 ml	2.6 ml
P-/BGM10	0.52	10	12.5 g	100 ml	6.5 ml

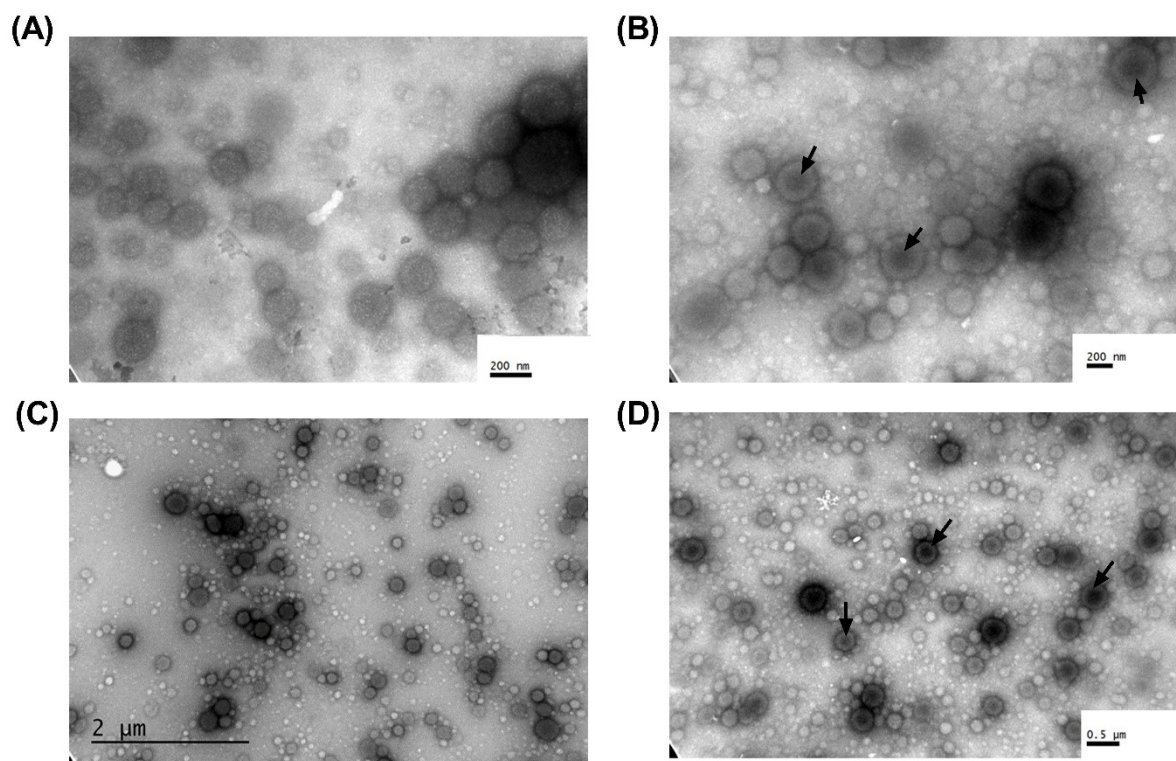
a: x molar ratio = mol MAA to mol unsubstituted amines



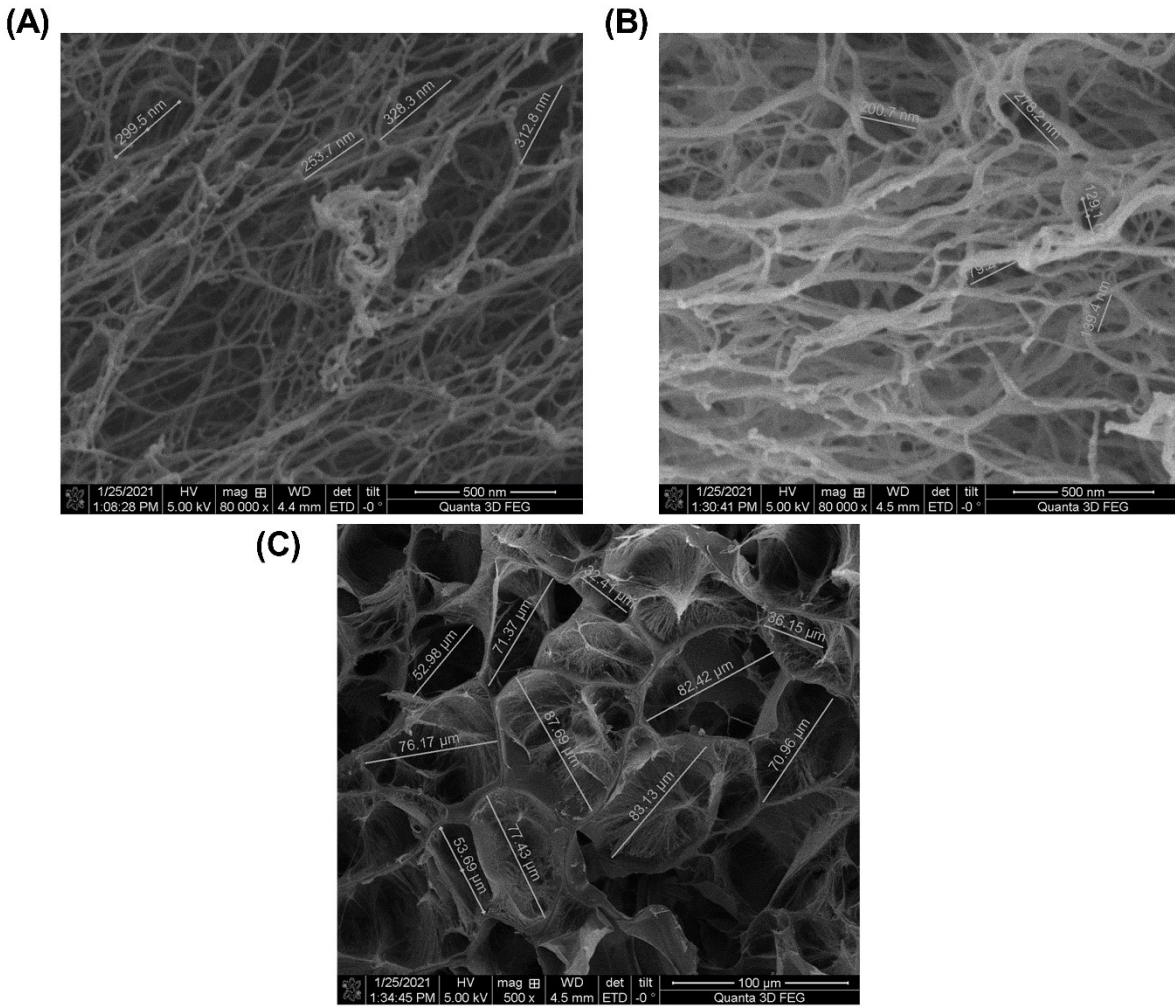
Supplementary Figure S1. (A) Changes in DM depend on the gelatin source and the excessive molar ratio of MAA to amino groups. (B) The amount of reactive functional groups in the side chain. The data on hydroxyl groups in PG and BG was obtained from a manufacturer’s reference, while the number of amino groups was calculated in this study using eq 1 with TMSP as an internal reference. Student’s t-test $*p < 0.001$



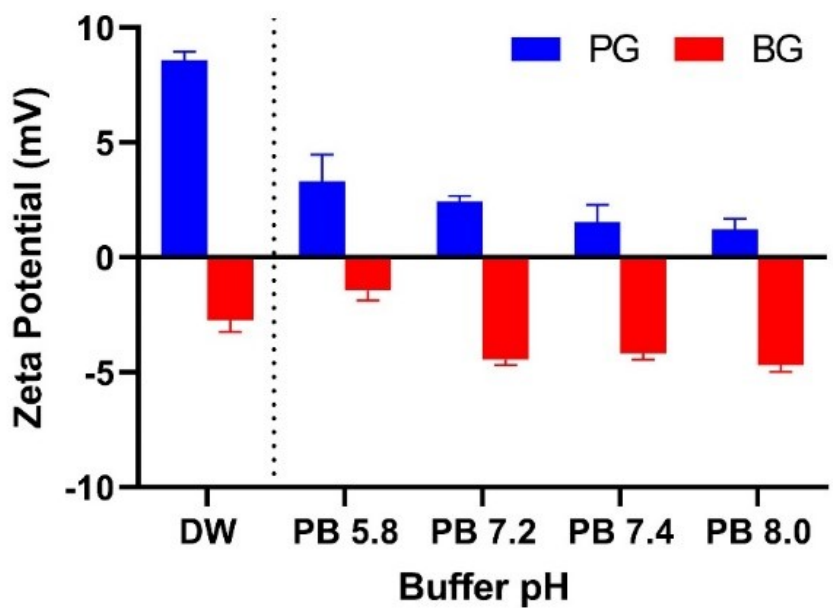
Supplementary Figure S2. (A) the proton NMR spectra of PG04 nanogels in different crosslinking degrees. (B) the proton NMR spectra of BG04 nanogels in different crosslinking degrees.



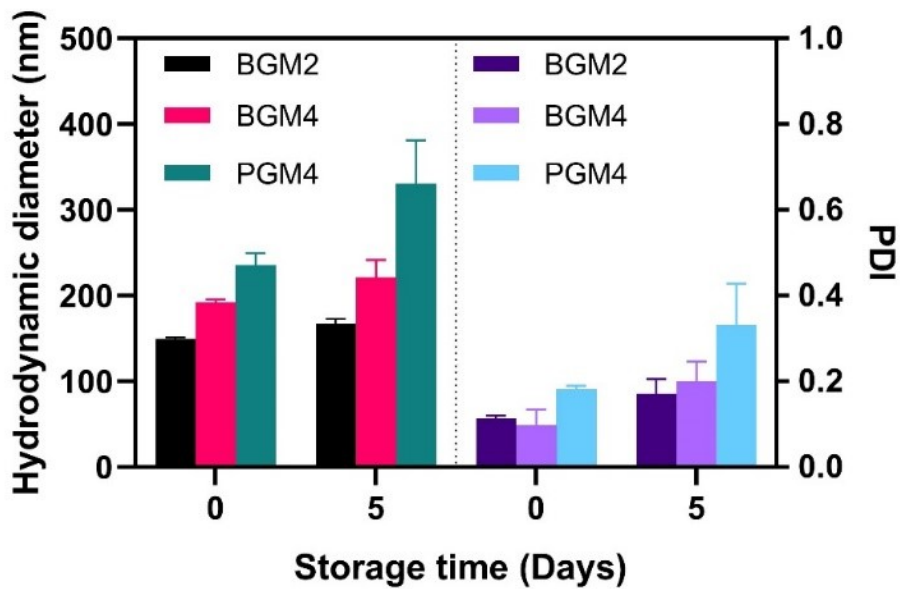
Supplementary Figure S3. Nanogels morphology using TEM. (A) photocrosslinked PG04 under UV irradiation (30 minutes); (B) Filaggrin-loaded PG04 (UV 30 minutes) nanogel dispersed in deionized water; (C) Naked BG04 nanogels (UV30) in PBS buffer (pH 7.4); (D) Filaggrin-loaded BG04 nanogels (UV30 minutes) in deionized water.



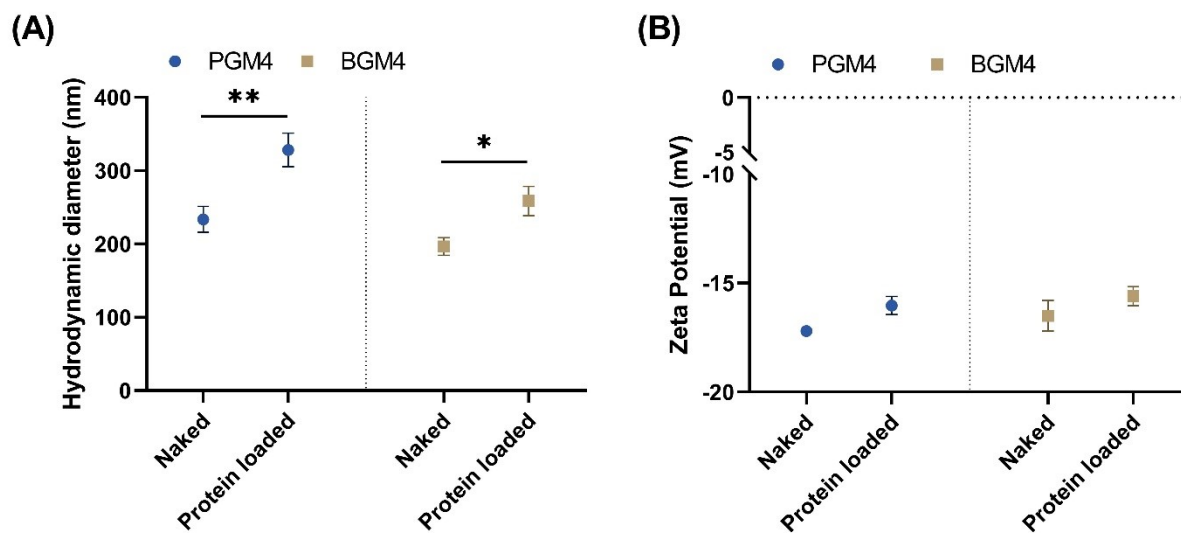
Supplementary Figure S4. GelMA microstructure (A) porous structure in BGM4. (B) and (C) microstructure of PGM4 (porous structure).



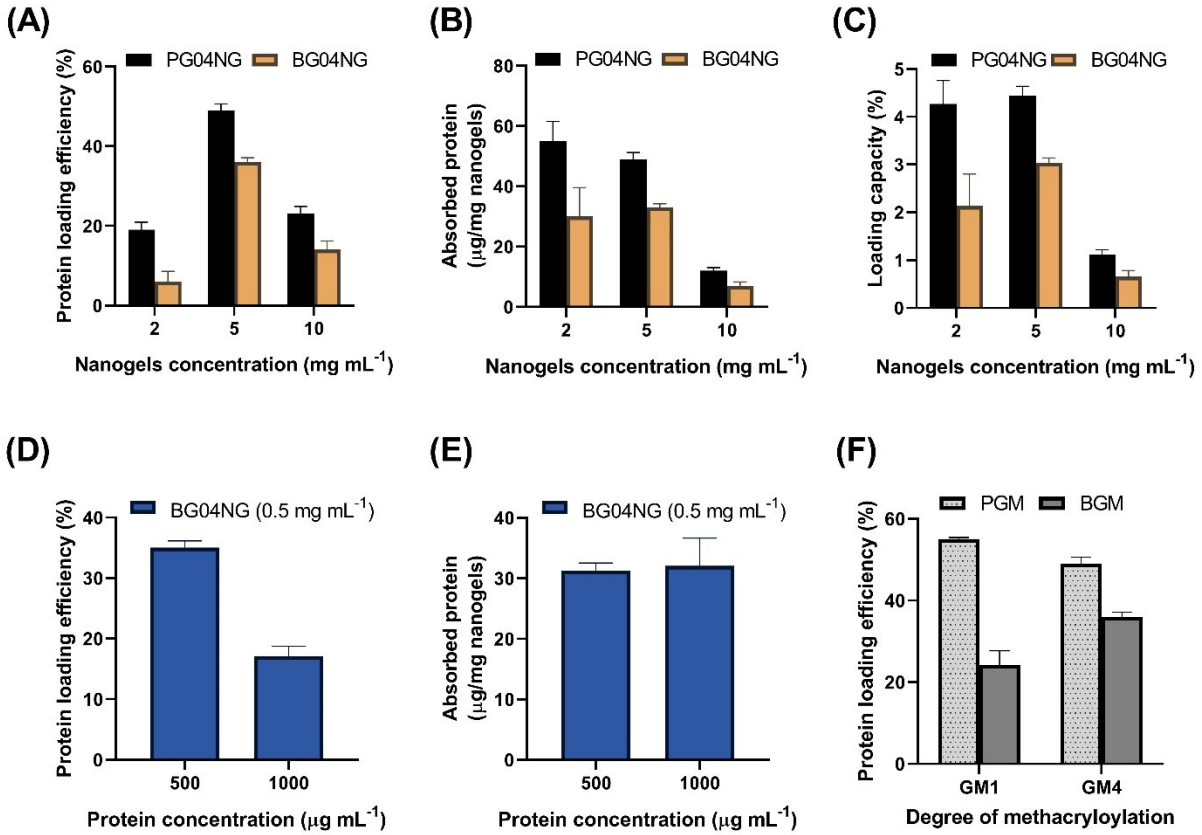
Supplementary Figure S5. The change in ζ -potential of gelatin (10 mg ml⁻¹) in solution. Mean \pm SD, n=3.



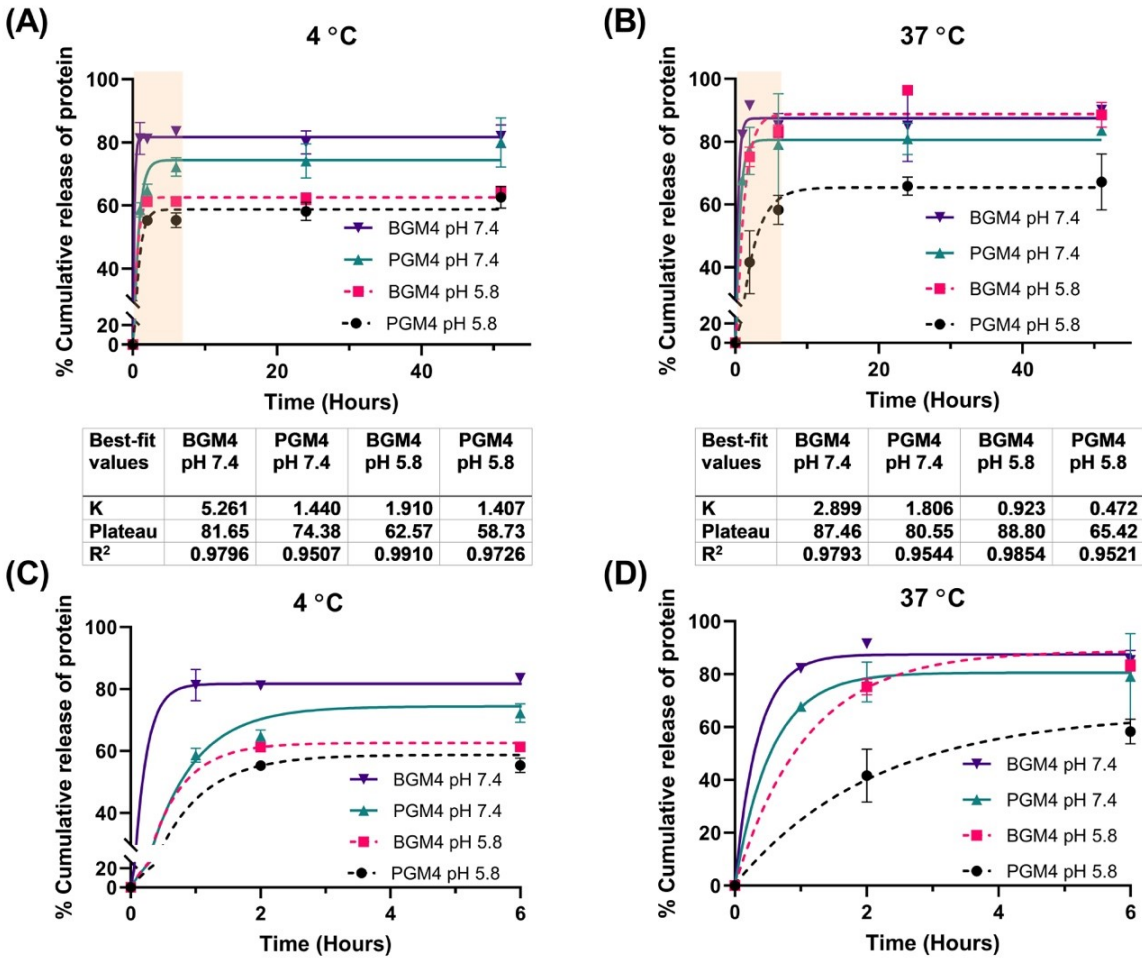
Supplementary Figure S6. The stability of the hydrated nanogels in deionized water (pH 7.4): The initial d_H and PDI measurement of fully swollen nanogels in solution and evolved d_H and PDI after 5 days of storage at 25 °C. PDI: polydispersity index. Mean \pm SD, n=3.



Supplementary Figure S7. The changes in d_H (A) and ζ -potential (B) before and after protein loading to PGM4 and BGM4 nanogels matrix. Mean \pm SD, n=3.



Supplementary Figure S8. Studies on % protein loading efficiency, degree of protein absorption, and loading capacity. Mean±SD, n=3.



Supplementary Figure S 9. Nanogels with low degree of protein absorption: initial D_{ab} of $(mNG-FLG)_{low}$ -PGM4 nanogels and $(mNG-FLG)_{low}$ -BGM4 nanogels were 12 μg per mg nanogels and 7 μg per mg nanogels, respectively. (Note that initial D_{ab} of the $(mNG-FLG)_{high}$ -PGM4 nanogels and $(mNG-FLG)_{high}$ -BGM4 nanogels were 49 μg per mg nanogels and 33 μg per mg nanogels) (A) the $(mNG-FLG)_{low}$ -PGM4 nanogels and $(mNG-FLG)_{low}$ -BGM4 nanogels incubated either in PB (pH 7.4) or in PB (pH 5.8) at 4 °C. In the first 24 hours, the nanogels were incubated in deionized water and then changed to PB. (B) the $(mNG-FLG)_{low}$ -PGM4 nanogels and $(mNG-FLG)_{low}$ -BGM4 nanogels incubated either in PB (pH 7.4) or in PB (pH 5.8) at 37 °C. In the first 24 hours, the nanogels were incubated in deionized water and then changed to PB. (C) The protein release profile from PGM4/ BGM4 nanogels in the first 6 hours after buffer change at 4 °C. (D)

The protein release profile from PGM4/ BGM4 nanogels in the first 6 hours after buffer change at 37 °C. Mean±SD, n=3.